

In-Line Wideband RF MEMS Switch Integrated on PCB Using BCB Planarization

I. C. Benitez-Zuñiga, A. E. Martynyuk, J. I. Martinez-Lopez and J. Rodriguez-Cuevas

Abstract—In this paper, the design, fabrication, and characterization of a wideband cantilever RF-MEMS coplanar line switch with metal-to-metal contact are presented. Printed circuit board (PCB) processing techniques and benzocyclobutene (BCB) as planarization material were used to integrate the RF-MEMS switch to a microwave-friendly substrate. The proposed fabrication process was developed at low-temperature ($< 210\text{ }^{\circ}\text{C}$) and combines layers of BCB, photoresist and copper. The process is relatively simple, comparatively inexpensive, and it implies a wide usage of BCB as planarization material to reduce the surface roughness of the cantilever beam, enabling a high repeatability of the fabricated MEMS switches. This low-cost fabrication process was used to develop a switch with low actuation voltage, and acceptable levels of insertion loss and isolation in the frequency band from DC to 20 GHz. The fabricated switch demonstrated isolation higher than 13.1 dB and insertion loss lower than 0.63 dB in the frequency range from DC up to 12 GHz. In frequencies from 12 to 20 GHz, the insertion loss is lower than 1.16 dB and the isolation is higher than 9.6 dB. The pull-in voltage was 30 V with measured commutation time of 425 μs . This RF-MEMS switch is suitable to be monolithically integrated with printed circuits on flexible microwave-friendly substrates.

Index Terms—Flexible printed circuits, Microelectromechanical systems, Microfabrication, Radiofrequency microelectromechanical systems.

I. INTRODUCTION

The RF-MEMS switch has been studied intensively due to its distinct advantages over conventional semiconductor and mechanical switches. RF-MEMS switches have demonstrated low insertion loss, higher isolation, and extremely low power consumption when compared with p-i-n diode or FET switches [1]–[4]. For these reasons, RF-MEMS switches are attractive in microwave low-loss circuits required in electronically reconfigurable active frequency selective surfaces (AFSS), phase shifters for phased arrays and reflectarrays, reconfigurable lenses, commutation networks for satellite communications, and Single-Pole N-Throw (SPNT) switches in portable units or base stations [4]–[12], among others.

Recently, reconfigurable reflectarrays and active frequency selective surfaces have been studied for their capability to adjust their responses to a varying dynamic scenario imposed by the new generation of wireless communication systems. However, one of the main obstacles of these 2-dimensional reconfigurable arrays is the large number of switching devices

that need to be embedded in the array to perform the reconfiguration (Fig. 1). These arrays are commonly fabricated on microwave-friendly substrates, therefore, the development of a low-cost RF switch that can be integrated to the PCB substrate during the fabrication stage is of primary importance to reduce manufacturing cost and time. Thus, it is highly desirable to develop a relatively simple and inexpensive fabrication process for the RF-MEMS switches.

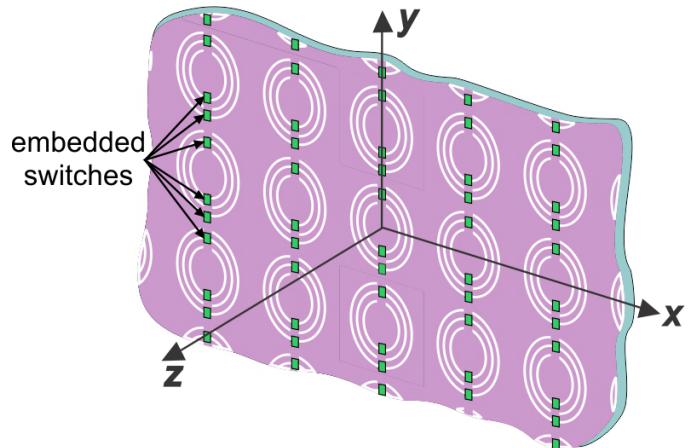


Fig. 1. Active frequency selective surface with monolithically integrated switches.

One of the technologies that has the potential to improve the above-mentioned features is known as Printed Circuit Board for MEMS (PCB-MEMS), where conventional PCB processing techniques and specialized micromachining techniques are combined [13]. The PCB technology provides an essential advantage of low-loss operation over standard monolithic technologies based on semiconductor substrates. This technology is suitable for monolithic integration of the RF-MEMS switches with other components on a single board, avoiding the expensive and time-consuming assembly process, typically used for hybrid integrated circuits.

However, an important issue in PCB-MEMS fabrication is the large copper cladding thickness of the substrate that affect the deposited layers of the MEMS structure. At high frequencies, the surface roughness in the metal bridges or cantilevers of the switches produces a detrimental effect both in the conductivity and in the surface impedance [14]. The strong surface roughness and relatively large thickness of the substrate metallization require special procedures and additional unconventional technological steps to obtain a good planarization during the fabrication process. These additional steps, such as forced planarization, electro-chemical polish-

This work was supported by the Programa de Apoyo a Proyectos de Investigación e Innovación Tecnológica de la Dirección General de Asuntos del Personal Académico (DGAPA-PAPIIT) under Grant IN118620, Grant IN119420, Grant IN111522, Grant IN105823 and Grant IN114823. I. C. Benitez-Zuñiga, A. E. Martynyuk, J. I. Martinez-Lopez, and J. Rodriguez-Cuevas are with the Universidad Nacional Autónoma de México. CdMx, 04510, México (e-mail: jorgerc@fi-b.unam.mx).

ing, and electro-plating, often compromise the reliability and repeatability of the fabricated devices and increase the fabrication costs.

Considerable research efforts in the development of RF-MEMS switches compatible with PCB technology as well as planarization techniques have been realized. The published works that have been mostly reported in the state-of-the-art review are the bridge-type and cantilever-type RF-MEMS switches. In [15], capacitive RF-MEMS shunt switches based on Kapton-E polyimide film are presented. The switches have good performance. However, the fabrication process is quite complex as it includes the lamination of various layers with a thermo-compression bonding of various layers of the switch and the micromachining of one of these layers with a milling machine. This results in a complex process, which implies an increase in the cost of manufacturing. Furthermore, the actuation voltage to control these devices is quite high, requiring additional electronic circuits to convert low voltages to high voltages. In [16], a low-temperature high-density inductively coupled chemical vapor silicon nitride deposition and compressive molding planarization are used to develop a capacitive type of RF-MEMS shunt switch. However, this technique could potentially compromise the devices repeatability since using the photoresist as a sacrificial material frequently results in the cantilever sticking unless, the supercritical drying technique is used. In [17], another planarization technique that comprises polishing the sacrificial layer is presented. The polishing of the surface with SiC leads to scratching of the polished polyimide, and the resulting copper layer presents cuts and scratches. Therefore, one needs a second polishing step achieved by using a diamond solution, which makes the process relatively expensive, and the repeatability of the switches also could be compromised. In [18], a RF-MEMS switch is fabricated using a transfer technology by first placing the switch on silicon substrate using a standard process and compatible materials. Then, the switch is transferred to a PCB substrate by a thermal process. Next, the wafer bonding is conducted under a specially designed process condition to avoid wafer warpage. Finally, to complete the process, the remaining Si, SiN, and the sacrificial oxide layers, must be removed through a complex and expensive technological step. In [19], a RF-MEMS switch with reduced actuation voltage is presented. The pull-in voltage (30 – 40 V) is relatively low as compared with the above-mentioned RF-MEMS switches. The reduction of the actuation voltage is achieved at the cost of additional technological steps and expensive materials such as titanium and gold. The fabrication process includes chemical-mechanical polishing, high-density inductively coupled plasma chemical vapor deposition, and electroplating. Furthermore, copper and photoresist are used as sacrificial layers, therefore the release process is complex, and the repeatability of the switches could be compromised. In [20], traditional PCB materials along with photolithographic high-density interconnect techniques were used to develop a cantilever-type RF-MEMS switch. The switch performance is competitive to silicon RF-MEMS using a low-cost fabrication process. However, the use of better photo-imageable dielectric materials will improve the performance and processability

of this technology. In [21], a RF-MEMS cantilever switch with electrostatic actuation and metal-to-metal contact on a microstrip transmission line is presented. The fabrication process is relatively simple and inexpensive. However, this switch demonstrates a high actuation voltage of 90 V.

From this brief literature review of PCB-MEMS technology, it is observed that the existing planarization problems in monolithically integrated MEMS switches that affect their cost, repeatability, and performance. Therefore, the main motivation of this work is to develop RF-MEMS switches with good planarization, satisfactory electrodynamic properties, low-actuation voltages, and low fabrication cost. The proposed switch accomplishes planarization of the cantilever beam based on benzocyclobutene (BCB). The developed fabrication process is relatively simple, comparatively inexpensive, and it implies a wide usage of BCB as planarization material to reduce the surface roughness of the cantilever beam, enabling a high repeatability of the fabricated devices. In this paper, we present the design, fabrication, and characterization of an in-line wideband RF-MEMS cantilever beam switch with metal-to-metal contact and electrostatic actuation integrated on a coplanar waveguide (CPW) and fabricated with PCB technology on a flexible microwave friendly substrate. The proposed technology might positively impact the advances in microwave circuits that use a large number of built-in switches, such as AFSS, reconfigurable antennas or phased arrays.

II. RF-MEMS DESIGN

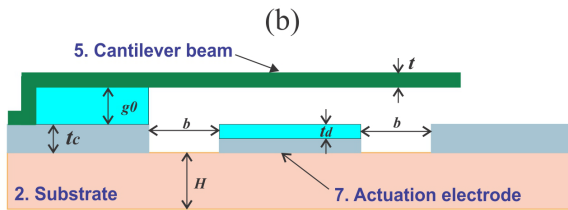
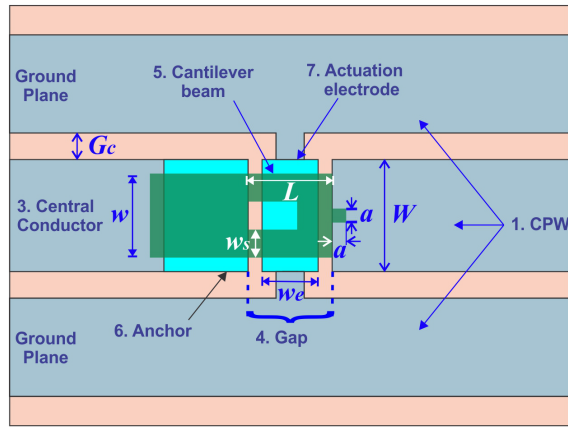
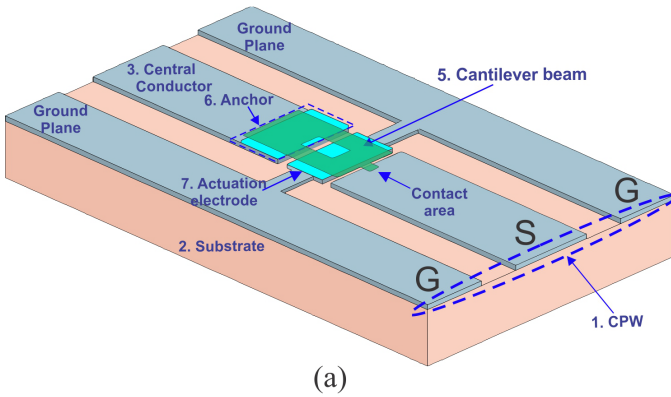
The proposed series-type RF-MEMS switch with a metal-to-metal contact is shown in Fig. 2 (a)-(c). This switch is integrated to a CPW 1, embedded on a microwave-friendly substrate 2.

The main element of the switch is a movable metal cantilever beam 5, with one end anchored to the central conductor 3 while the other end is free. When the switch is in the OFF state, the free end of this cantilever beam is suspended above the central conductor with an initial gap g_0 . Therefore, the continuity of the central conductor 3 is interrupted, which prevents the transmission of the RF signal across the coplanar waveguide 3.

The commutation to the ON state occurs when a control voltage is applied between the cantilever beam and the actuation electrode 7. The electrostatic force applied to the cantilever beam causes a deflection of the free end over the central conductor. Thus, a metal-to-metal contact of a protruding feature that represents the contact area and the central conductor is achieved enabling the continuity of the RF signal through the central conductor of the CPW.

The essential RF-MEMS switch's parameters that determine its performance are the actuation voltage, the insertion loss, the isolation, and the operational band. The cantilever beam switch ensures a lower spring constant as compared to typical spring constants for bridge-type switches and, consequently, a lower actuation voltage. Furthermore, MEMS switches with direct metal-to-metal contact operate in a wider frequency band with lower insertion loss as compared to capacitive MEMS switches. In this design, to ensure a proper operation of the

switch, the selected constructive material for the cantilever beam is copper as it ensures compatibility with the fabrication process as well as providing adequate stiffness that guarantees simultaneously low actuation voltage and the proper restoring force sufficient to subdue the stiction.



(c)

Fig. 2. Schematic configuration of the In-Line Wideband RF-MEMS Switch Integrated on PCB Using BCB Planarization. (a) Perspective view (b) Top view (c) Transversal view.

Benzocyclobutene (BCB) photodefinable polymer is extensively used in planar millimeter wave structures due to the low dielectric constant (2.65), low loss tangent (0.0008 at 10 GHz) and the excellent planarization characteristics that are fundamental to overcome the roughness of the microwave substrate metal cladding [22]–[25].

The ability to planarize topographical conductor features of the BCB have been used, with a degree of planarization (DOP) up to 95% to make electrically and mechanically more stable conductors due to the outstanding topographical leveling [24], [25].

The cantilever beam is partially anchored on a BCB layer with thickness of $5 \mu\text{m}$ to ensure a stable gap between the cantilever and the control electrode 7. On the other hand, the actuation electrode is covered by a thin ($1 \mu\text{m}$) BCB layer to avoid a short circuit between the cantilever beam and the actuation electrode in the ON state. Note that the planarization of the cantilever beam is achieved both in its anchored section as well as in the section above the actuation electrode.

RF-MEMS switches are mainly characterized by a set of essential parameters such as actuation voltage, commutation time, isolation, insertion loss, and return loss. The geometry and sizes of the RF-MEMS switch were optimized using both MEMS-specific multi-physics solvers within CoventorWare® and 3D EM analysis solvers within CST Studio Suite® to obtain a good balance in the above-mentioned parameters in a large operating frequency band (0.5-20 GHz). The optimized sizes of the switch's geometry are shown in Table I.

TABLE I
SIZES OF THE IN-LINE WIDEBAND RF-MEMS SWITCH
INTEGRATED ON PCB USING BCB PLANARIZATION

Symbol	Description	Quantity
g_0	Initial gap	$5 \mu\text{m}$
w	Width of the beam	$300 \mu\text{m}$
w_s	Width of the non-meandered beam	$100 \mu\text{m}$
w_e	Width of the electrode	$200 \mu\text{m}$
t	Thickness of the beam	$1 \mu\text{m}$
L	Length of the beam	$300 \mu\text{m}$
t_d	Thickness of the dielectric layer	$1 \mu\text{m}$
W	Width of the central conductor of the CPW	$400 \mu\text{m}$
G_c	Gap of the CPW	$195 \mu\text{m}$
t_c	Thickness of the CPW lines	$11 \mu\text{m}$
a	Length of the square contact area	$50 \mu\text{m}$
b	Gap between the central conductor and the actuation electrode	$50 \mu\text{m}$
H	Thickness of the substrate	$127 \mu\text{m}$

III. ELECTROMECHANICAL ANALYSIS

A. Actuation Voltage

The equivalent mechanical structure of the RF-MEMS Cantilever switch is shown in Fig. 3 (a). When a DC voltage V is applied between the actuation electrode and the movable membrane, an electrostatic force F_e is developed on the cantilever beam. The dependence of the applied voltage V and the cantilever deflection g has been developed in [26].

$$V = \sqrt{\frac{2k(g_0 - g)(g + \frac{t_d}{t_r})^2}{\epsilon_0 A}} \quad (1)$$

The increase of the applied voltage V leads to the reduction of the gap g due the increment of the electrostatic force. Then, at approximately $(2/3)g_0$, the electrostatic force significantly overtakes the restoring force. Thus, the position of the beam becomes unstable leading to the collapse of the cantilever

beam. When the applied voltage increases to reach the pull-in voltage, the membrane collapses to the actuation electrode ensuring the ON state of the switch. The pull-in voltage is calculated at $g = (2/3)g_0$. The mechanical simulations of the proposed switch are shown in Fig. 4. The dependence of the gap g as a function of the applied voltage V is calculated and shown in Fig. 5. For comparison purposes, the same dependence, simulated with the help of CoventorWare, is also presented. One can observe a good agreement between calculated and simulated curves.

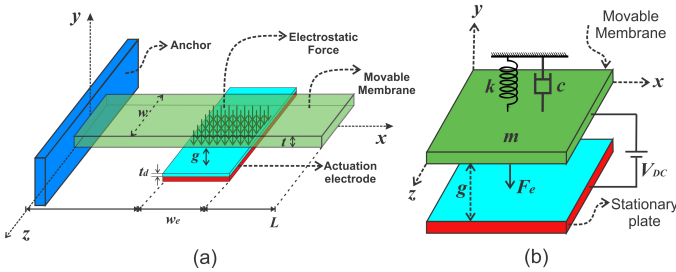


Fig. 3. a) Schematic diagram of the In-Line Wideband RF-MEMS Switch Integrated on PCB Using BCB Planarization, and b) dynamic electromechanical model of the proposed switch.

B. Commutation Time

To calculate the commutation time, the cantilever beam was modelled as a system of parallel plates separated by the initial gap g_0 with a movable upper plate of mass m and area A , suspended by a spring of stiffness k , and a damper with damping coefficient c . This dynamical electromechanical model is shown in Fig. 3 (b) with the following parameters: $m = 1.577E-10$ g, $k = 1.7725$ N/m, and $c = 4.129E-04$ Ns/m. The calculation of the system response can be performed applying d’Alembert’s principle [26], leading to the inhomogeneous second-order ordinary differential equation. It is worth mentioning that this differential equation is non-linear, and the solution requires complicated numerical analysis. Several works have reported computational approximations using methods as Boundary Element Method, Finite Element Method, and LaGrangian Schemes to predict the dynamic behavior of the electrostatic actuated MEMS [27]–[29]. In this work, CoventorWare was used to obtain the commutation time. The time response is shown in Fig. 6, where one can observe a commutation time around $400 \mu s$.

IV. FABRICATION PROCESS

A surface micromachining fabrication process over a flexible microwave friendly substrate is proposed. This process is developed at low-temperature ($< 210 \text{ }^\circ\text{C}$) and combines layers of BCB, photoresist and copper. The geometry of the designed RF-MEMS switch is shown in Fig. 2. The first step comprises the patterning of a CPW with characteristic impedance of 50 Ohm on the copper cladding of the Rogers RO5880 substrate, with a dielectric thickness of 0.127 mm. Next, two thin-film isles of photosensitive benzocyclobutene (BCB) were patterned, the first one ($1 \mu m$ thickness) was

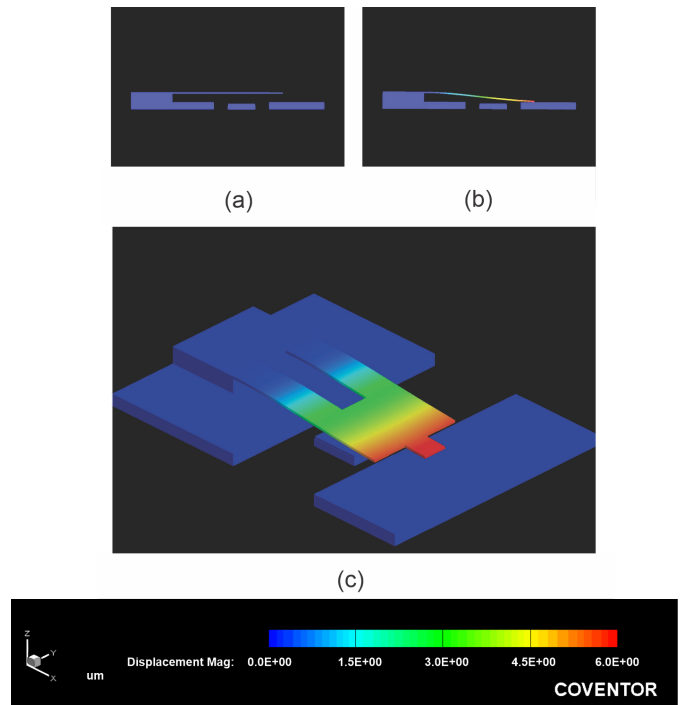


Fig. 4. Electromechanical simulations of the In-Line Wideband RF-MEMS switch. a) side view of the OFF state, b) side view of the ON state, and c) perspective view.

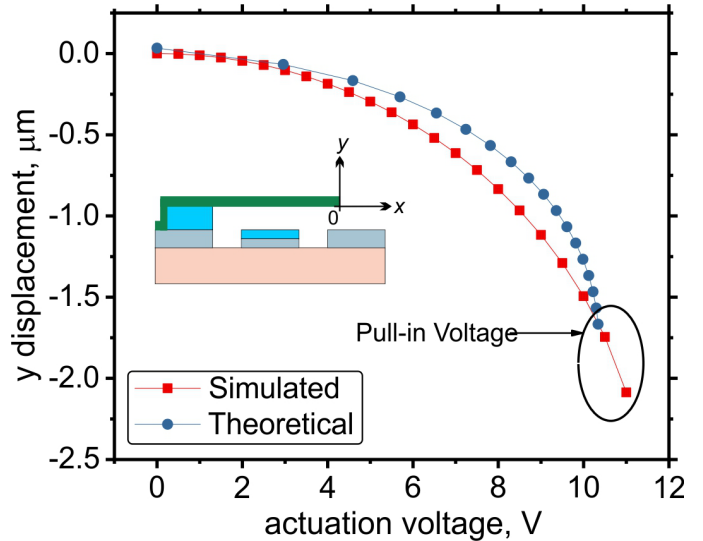


Fig. 5. Displacement of the cantilever beam when an actuation voltage is applied.

defined to avoid a short circuit between the cantilever and the actuation electrode, and the second one ($5 \mu m$ thickness), was used to anchor the cantilever beam on the fixed end. Thus, one part of the copper cantilever beam is anchored to the BCB isle of $5 \mu m$, meanwhile the free end of the cantilever beam is suspended over the other side of the CPW conductor setting a gap g_0 of $5 \mu m$.

Fig. 7 (a)-(h) shows the fabrication process flow of the switch. The process starts by etching the copper clad of the microwave-friendly substrate to reduce its thickness from 17 to $11 \mu m$ to obtain a better resolution in the subsequent steps

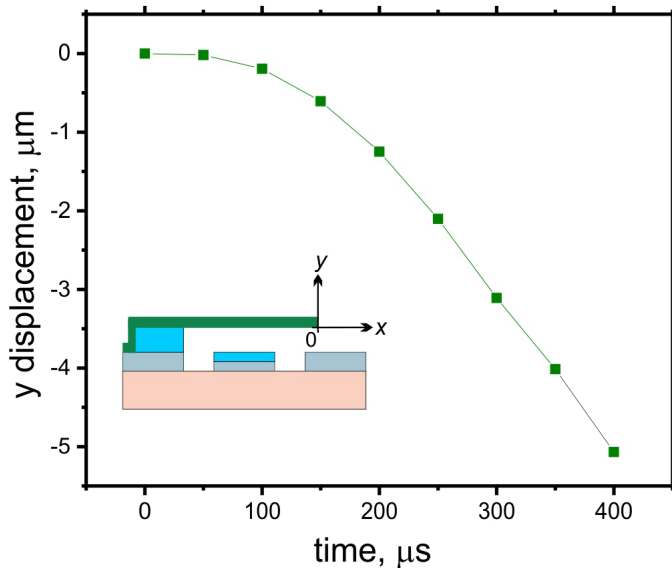


Fig. 6. Calculated transient characteristic of the cantilever beam.

(Fig. 7(a)). Next, this copper was patterned to form the central conductor and the ground planes of the CPW, as well as the actuation electrode of the switch (Fig. 7(b)). To avoid a short circuit with the actuation electrode when the cantilever beam pulls-down, it is necessary to decap the area of the actuation electrode by etching $1\ \mu\text{m}$ of copper (Fig. 7(c)) to further fill it with a $1\ \mu\text{m}$ -thick film of BCB. As our process uses positive photoresist (AZ9245), the respective photomask allows only ultraviolet (UV) exposure to the actuation electrode area, protecting the rest of the switch and the CPW. The actuation electrode etching was performed using an etchant based on hydrogen peroxide/hydrochloric acid/water solution during a time of 4 seconds, required to remove $1\ \mu\text{m}$ -thick of copper. The next step is the deposition and patterning of a $5\ \mu\text{m}$ -thick BCB layer to form the anchor of the cantilever (Fig. 7(d)). The UV exposition was adequate to initially polymerize the BCB. Then the BCB film was cured at a temperature of 210°C for 40 min and after this curing, the first BCB layer becomes chemically and mechanically stable. Thus, this BCB film cannot be damaged by subsequent lithographic steps. The same procedure was performed to cover the actuation electrode (Fig. 7(e)) with a $1\ \mu\text{m}$ -thick film of BCB. The thickness of the BCB layers was determined by the angular speed and time of the spin-coating deposition steps. The $1\ \mu\text{m}$ -thick BCB layer (Dow XU-35133) required a speed of 3500 rpm for 30 seconds, while for the $5\ \mu\text{m}$ -thick layer (Dow 4024-40), a speed of 2000 rpm and 30 seconds was used. Subsequently, the photoresist was deposited and patterned to form a sacrificial layer (Fig. 7(f)). Next, a $1\ \mu\text{m}$ -thick copper film was deposited using the RF sputtering technique. This copper film was patterned to form the switch membrane (Fig. 7(g)). Finally, the structure was released (Fig. 7(h)) using a supercritical dryer to avoid stiction. A photograph of the fabricated RF MEMS switch is shown in Fig. 8.

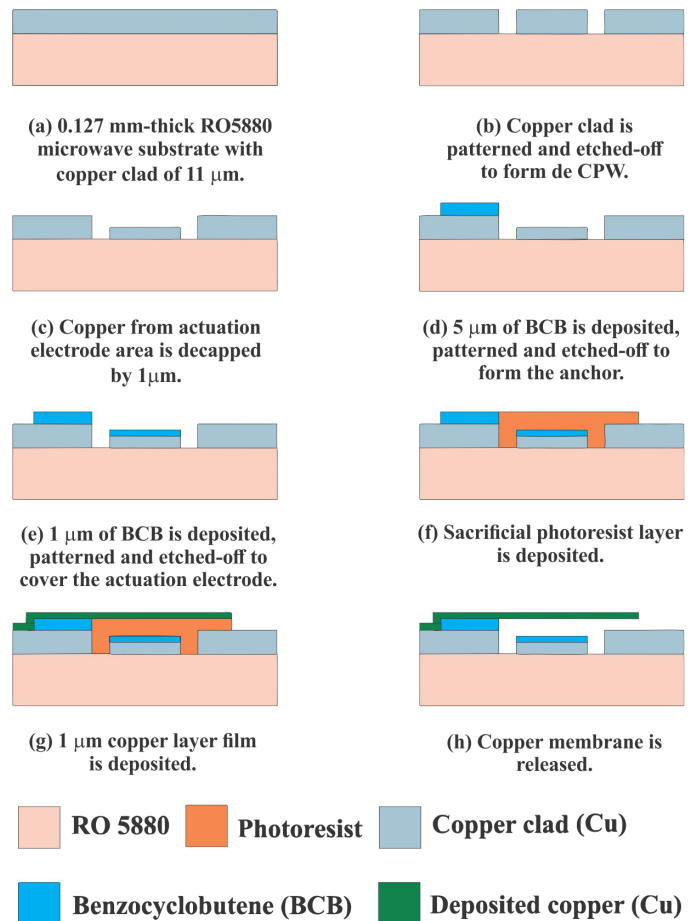


Fig. 7. Fabrication process flow for the proposed RF-MEMS switch.

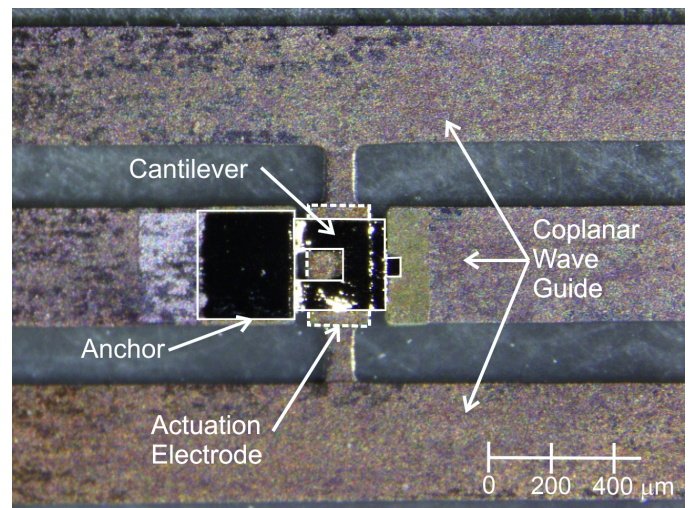


Fig. 8. Photograph of the fabricated In-Line Wideband RF-MEMS Switch Integrated on PCB Substrate using BCB Planarization. Note that at the top and bottom of the figure, the CPW ground planes (copper) are shown. The darker parts are the gap between the ground planes and the center conductor.

V. ELECTROMECHANICAL EXPERIMENTAL RESULT

The electromechanical characterization of the fabricated RF MEMS switch was obtained. The fabricated switch was actuated using a probe station. Initially, the pull-in voltage of

switch was measured. Next, the commutation time is obtained. A voltage source is configured to create a unipolar square wave with minimum and maximum values of 0 and 30 V, respectively. The low value of this square signal removes the electrostatic force between the actuation electrode and the cantilever beam enabling the OFF state of the switch, while the high value of the square wave introduces the electrostatic force to produce the downward actuation. The change between these two values is used to measure the actuation time of the switch. An AC waveform generator creates a 10-KHz sinewave that travels across the CPW in the ON state.

The measured voltages at the actuation terminals and the output of the switch are shown in Fig. 9. The rising edge of the square wave causes the deflection of the cantilever beam, and the switch goes from the OFF to the ON state. Thus, the injected AC signal at the input of the switch will appear after some delay at the output of the switch. Note, that the time delay between the pulse and the AC signal at the output of the switch was measured as the interval between the instant when the step signal settles the actuation voltage and the instant when the AC signal appears at the output of the switch as shown in Fig. 9. The measured actuation voltage was 30V and the measured commutation time was 425 μ s. Table II shows the theoretical, simulated, and experimental values of the switch's pull-in voltage and commutation time. A large difference is observed between simulated and measured results in the pull-in voltage. This issue has also been reported in [17]. Several factors can be attributed to affecting this parameter such as differences in the air gap height due to fabrication discrepancies, as well as changes in the copper Young's modulus due to external contamination of the fabricated 1 μ m-thick thin film cantilever beam.

TABLE II
DEVICE PARAMETERS: THEORETICAL, SIMULATED AND MEASURED RESULTS

Parameter	Theoretical	Simulated	Measured
Actuation Voltage	10 V	11 V	30 V
Commutation time	Not calculated	400 μ s	425 μ s

VI. RF MODELLING AND CHARACTERIZATION

A. RF Modelling

The equivalent circuit models for the OFF and ON states of the proposed switch are shown in Fig. 10 (a) and (b), respectively. Two transmission lines with characteristic impedance Z_0 correspond to the two sections of the CPW at the input and output of the switch. The inductance of the cantilever is represented by L . The resistor R is used to take into account the conductive losses of the cantilever beam. In the OFF state, the capacitor C_u models the parallel plate capacitance between the actuation electrode and the cantilever beam, while the capacitor C corresponds to the capacitive effect between the membrane protruding and the output section of the CPW. In the ON state, C is short-circuited by the collapsed membrane, and the capacitance between the membrane and the actuation

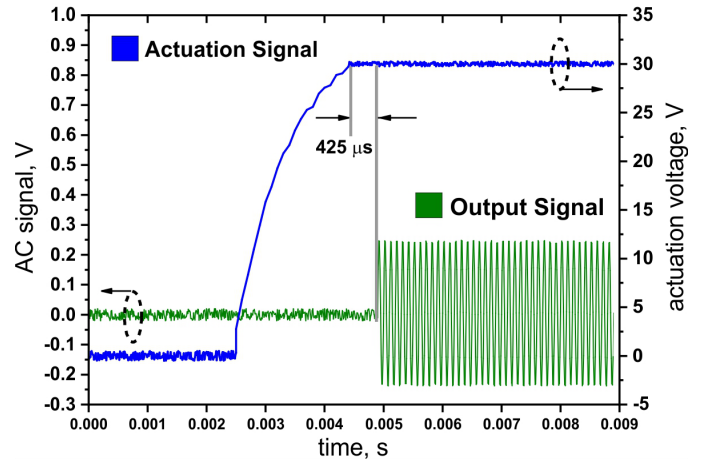


Fig. 9. Experimental results for testing the commutation time of the proposed RF-MEMS switch.

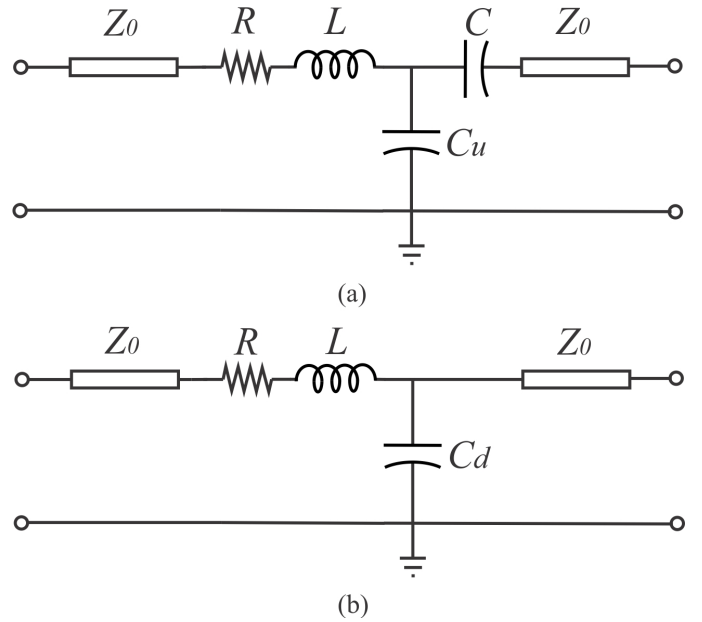
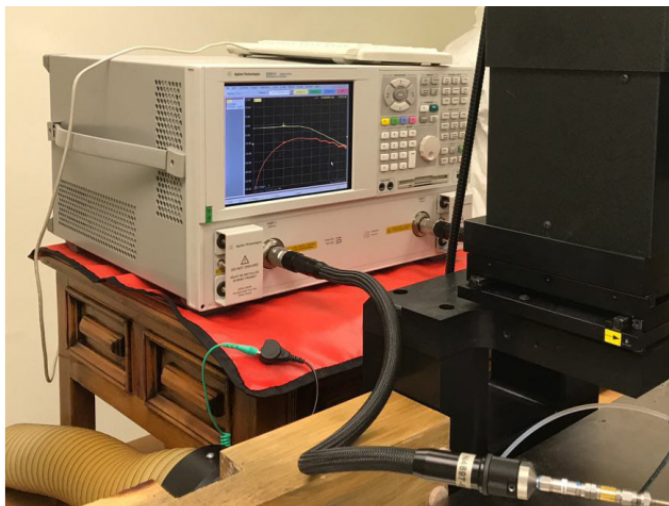


Fig. 10. Equivalent circuit model of the RF-MEMS switch. (a) OFF state, and (b) ON state.

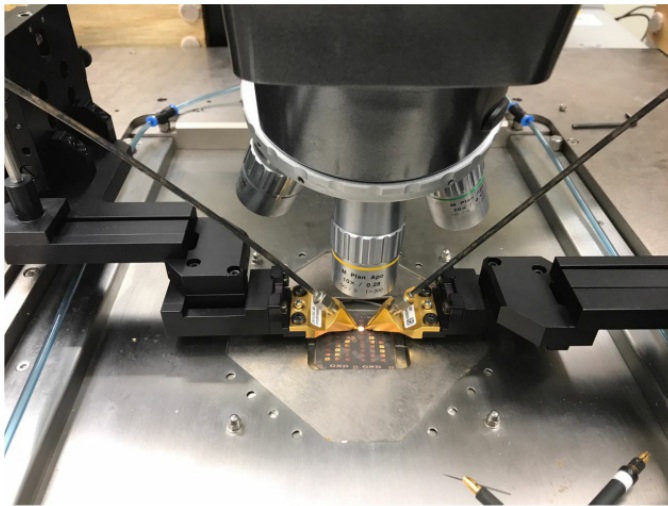
electrode increases due to the smaller distance between the cantilever and the actuation electrode. Thus, instead of C_u , a new capacitance value of C_d is included in the equivalent circuit for the ON state.

B. Characterization

The RF characterization of the proposed switch was obtained by measuring the insertion loss and return loss for the ON state, and isolation for the OFF state. When the switch is in the ON state (the cantilever beam of the switch is pulled down to contact with the CPW's central line), an RF signal passes through the transmission line with minimal insertion loss. On the other hand, when the switch is in the OFF state (the cantilever beam of the switch is pulled up), the path of the RF signal is blocked by the air gap between the free end of the cantilever beam and the central conductor of the CPW.



(a)



(b)

Fig. 11. Experimental setup of the electrodynamic characterization. a) VNA connected to the RF probe station, and b) fabricated switches tested using wafer probes.

TABLE III
MEASURED RF PARAMETERS

Frequency band	Maximum insertion loss dB	Minimum isolation dB
L	0.52	30.65
S	0.56	24.00
C	0.63	17.26
X	0.63	13.18
Ku	0.94	9.75

The scattering parameters of the fabricated RF-MEMS switches were characterized with an Agilent E8361A PNA network analyzer. A SUSS MicroTec PM8 probe station with the help of two Z40-X-GSG-500 Cascade MicroTec wafer probes were used to connect the input and output sections of the CPW as shown in Fig. 11. The S-parameters were measured

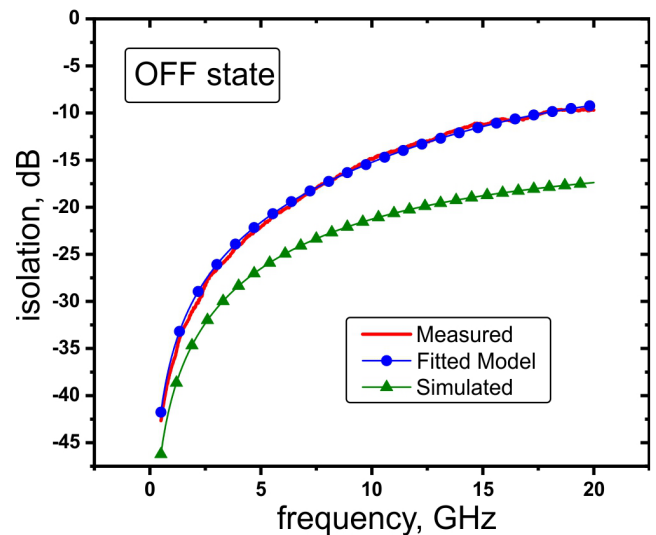


Fig. 12. Measured and simulated isolation of the switch in the OFF state.

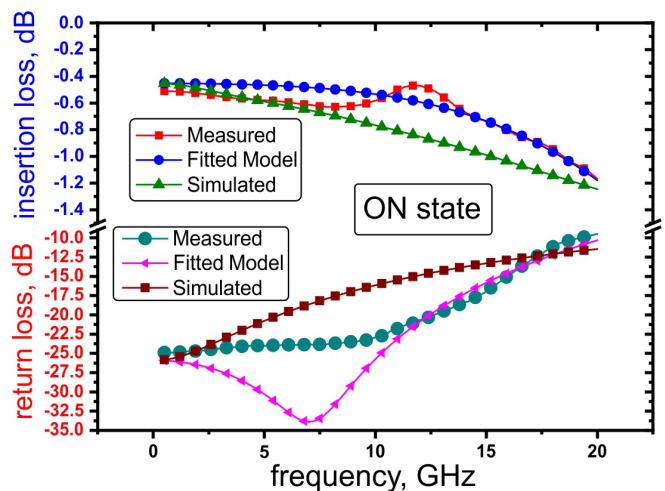


Fig. 13. Measured and simulated insertion loss and return loss if the switch in the ON state.

in the frequency interval from 0.5 to 20 GHz. The results for different microwave frequency bands are summarized in Table III. The fitted parameters of the switch are $R=5 \Omega$, $L=0.36 \text{ nH}$, $C_1 = 26 \text{ fF}$, $C_u = 110 \text{ fF}$, and $C_d = 140 \text{ fF}$. For comparison purposes, the same dependences were obtained from the equivalent circuit, the full-wave simulation using Microwave CST Studio Suite and the measured data. These results are shown in Fig. 12 and 13. Fig. 12 presents the isolation for the OFF state, and Fig. 13 shows the insertion loss and the return loss in the ON state.

A comparison of the proposed switch with other reported RF-MEMS switches based on PCB technology is presented in Table IV. The proposed RF-MEMS switch demonstrates low actuation voltage and a competitive performance at RF and microwave frequencies with respect to the same fabrication technology. The main advantage of this switch is the relatively simple fabrication process based on standard photolithography steps and BCB planarization that results in

TABLE IV
COMPARISON WITH STATE-OF-THE-ART RF-MEMS SWITCHES INTEGRATED ON PCB

Parameters / Reference	[15]	[16]	[17]	[18]	[19]	[20]	[21]	This work
Pull-in voltage, V	100-120	30	Not reported	35	30 - 40	30	90	30
Commutation time μ s	Not reported	120	Not reported	Not reported	Not reported	100	Not reported	425
Type of switch	Bridge	Bridge	Bridge	Bridge	Bridge	Cantilever	Cantilever	Cantilever
Bandwidth GHz	8 - 30	8 - 20	5 - 15	8 - 20	1.8 - 18	0 - 10	10 - 14	0.5 - 20
Insertion loss, dB	< 0.4	< 0.3	< 0.085	< 0.2	< 2	0.3	2.5	<1.16
Isolation, dB	> 10	> 13	> 12.5	> 7.5	> 9.8	> 22	> 8.7	>9.6
Fabrication complexity	High	Medium	High	High	High	High	Medium	Low
Fabrication Cost	High	Low	High	High	High	High	Low	Low
Planarization technology	Thermocompression bounding of layers	Compressive Molding	Polishing polyimide	Transfer technology	Spin-coating and polishing	Not reported	Spin-coating of photoresist	Spin-coating of BCB

a low-cost fabrication of the RF-MEMS switch, and the easy monolithic integration in reconfigurable devices that require multiple built-in switches.

VII. CONCLUSION

The design, fabrication and characterization of a RF-MEMS switch using BCB as planarization material and standard low-complex patterning-photolithography steps are presented in this paper. The RF-MEMS switch was monolithically integrated to a CPW printed on standard RO5880 substrate using PCB techniques. The presented RF-MEMS switch has good RF and electromechanical behaviors in a wide frequency band.

The switch shows good electromechanical and RF performances, with a low actuation voltage of 30 V and a commutation time around of 425 μ s. The insertion loss is lower than 0.47 dB and the isolation is higher than 13.1 dB in the band from DC to 12 GHz. In the band from 12 to 20 GHz, the insertion loss is lower than 1.16 dB and the isolation is higher than 9.6 dB. The developed fabrication process provides the advantage of low-complex planarization with the help of the BCB without complex and expensive technology steps, and the capacity of the monolithic integration with RF and microwave subsystems. Thus, the switches based on the developed process can be used for the fabrication of multibit phase shifters, reconfigurable reflectarrays, and active frequency selective surfaces, where a considerable number of switches is required.

REFERENCES

- [1] S. Lucyszyn, *Advanced RF Memes*. Cambridge University Press, 2010.
- [2] C. D. Patel and G. M. Rebeiz, "An rf-mems switch with mn contact forces," in *2010 IEEE MTT-S International Microwave Symposium, Anaheim, CA, May 2010*, pp. 1242–1245.
- [3] S. Mansoor and A. A. Khan, "Rf mems capacitive switch with high isolation for 5g communication," in *2019 Int. Conf. Commun. Techn. (ComTech), Rawalpindi, Pakistan, Apr. 2019*, pp. 1–3.
- [4] Z. Gong, Y. Zhang, X. Guo, and Z. Liu, "Multi-contact radiofrequency microelectromechanical systems switch with power divider/combiner structure for high power applications," *Micro Nano Lett.*, vol. 13, no. 8, pp. 1075–1078, 2018.
- [5] R. Ramadoss, A. Sundaram, and L. M. Feldner, "Rf mems phase shifters based on pcb mems technology," *Electron. Lett.*, vol. 41, no. 11, pp. 654–656, 2005.
- [6] Y. Luo, J. Xu, G. Yang, and H. Toshiyoshi, "Em radiation from electrostatic nonlinear pull-in instability of mems," *Electron. Lett.*, vol. 54, no. 2, pp. 68–70, 2018.
- [7] A. Morankar and R. Patrikar, "Dual frequency mems resonator through mixed electrical and mechanical coupling scheme," *IET Circuits, Devices Syst.*, vol. 12, no. 1, pp. 88–93, 2018.
- [8] H. Salti, E. Fourn, R. Gillard, E. Girard, and H. Legay, "" pharmacist cross" phase-shifting cell loaded with mems switches for reconfigurable reflectarrays," in *Proc. Eur. Conf. on Antennas and Propagation EuCAP 2010, Barcelona, Spain, Apr. 2010*, pp. 1–4.
- [9] C. Wang, X.-l. Guo, W.-x. Ou-Yang, Y.-h. Zhang, and Z.-s. Lai, "A novel tunable low-pass filter based on mems and cpw," in *Proc. Int. Conf. Electron. Meas. Instrum., Beijing, China, Aug. 2009*, pp. 4–687.
- [10] S. V. Hum and J. Perruisseau-Carrier, "Reconfigurable reflectarrays and array lenses for dynamic antenna beam control: A review," *IEEE Trans. Antennas Propag.*, vol. 62, no. 1, pp. 183–198, 2013.
- [11] S. Dey, S. K. Koul, A. K. Poddar, and U. Rohde, "Rf mems switches, switching networks and phase shifters for microwave to millimeter wave applications," *ISSS J. Micro Smart Syst.*, vol. 9, no. 1, pp. 33–47, 2020.
- [12] B. Prudhvi Nadh, B. Madhav, M. Siva Kumar, T. Anil Kumar, M. Venkateswara Rao, and S. Mohan Reddy, "Mems-based reconfigurable and flexible antenna for body-centric wearable applications," *J. Electromagn. Waves Appl.*, pp. 1–15, 2022.
- [13] B. A. Cetiner, J. Qian, H. Chang, M. Bachman, G. Li, and F. De Flaviis, "Monolithic integration of rf mems switches with a diversity antenna on pcb substrate," *IEEE Trans. Microw. Theory Techn.*, vol. 51, no. 1, pp. 332–335, 2003.
- [14] A. Karmakar, B. Biswas, and A. Chauhan, "Investigation of various commonly associated imperfections in radiofrequency micro-electromechanical system devices and its empirical modeling," *IEEE J. Microelectromech. Syst.*, pp. 1–10, 2021.
- [15] R. Ramadoss, S. Lee, Y. Lee, V. Bright, and K. Gupta, "Rf-mems capacitive switches fabricated using printed circuit processing techniques," *J. Microelectromech. Syst.*, vol. 15, no. 6, pp. 1595–1604, 2006.
- [16] H.-P. Chang, J. Qian, B. A. Cetiner, F. De Flaviis, M. Bachman, and G. Li, "Design and process considerations for fabricating rf mems switches on printed circuit boards," *J. Microelectromech. Syst.*, vol. 14, no. 6, pp. 1311–1322, 2005.
- [17] B. Ghodsian, C. Jung, B. A. Cetiner, and F. De Flaviis, "Development of rf-mems switch on pcb substrates with polyimide planarization," *IEEE sens. J.*, vol. 5, no. 5, pp. 950–955, 2005.
- [18] Q. Zhang, A. Yu, L. Guo, R. Kumar, K. Teoh, A. Liu, G. Lo, and D.-L. Kwong, "Rf mems switch integrated on printed circuit board with metallic membrane first sequence and transferring," *IEEE Electron Device Lett.*, vol. 27, no. 7, pp. 552–554, 2006.
- [19] M. Silva, S. Barbin, and L. Kretly, "Fabrication and testing of rf-mems switches using pcb techniques," in *Proc. IEEE MTT-S Int. Microw. Optoelectron. Conf., Belem, Brazil, Nov. 2009*, pp. 96–100.
- [20] K. Lian, M. Eliacin, R. Lempkowski, M. Chason, M. O'Keefe, and J. Drewniak, "Rf-mems switches on a printed circuit board platform," *Circuit World*, 2010.
- [21] C. Aguilar-Armenta and S. Porter, "Cantilever rf-mems for monolithic integration with phased array antennas on a pcb," *Int. J. Electr.*, vol. 102, no. 12, pp. 1978–1996, 2015.
- [22] *CYCLOTENE Advanced Electronic Resins [Online]*. Available: <https://wiki.nanotech.ucsb.edu/w/images/7/72/BCB-cyclotene-3000-revA.pdf> Accessed: 2022-02-01.
- [23] S. Costanzo, I. Venneri, G. Di Massa, and A. Borgia, "Benzocyclobutene as substrate material for planar millimeter-wave structures: dielectric

characterization and application," *J. Infrared Millim. Terahertz Waves*, vol. 31, no. 1, pp. 66–77, 2010.

- [24] T. Stokich, C. Fulks, M. Bernius, D. Burdeaux, P. Garrou, and R. Heistand, "Planarization with cyclotene™ 3022 (bcb) polymer coatings," *Mater. Res. Soc. Symp. Proc. MRS Online Proceedings Library (OPL)*, vol. 308, 1993.
- [25] D. Burdeaux, P. Townsend, J. Carr, and P. Garrou, "Benzocyclobutene (bcb) dielectrics for the fabrication of high density, thin film multichip modules," *J. Electron. Mater.*, vol. 19, no. 12, pp. 1357–1366, 1990.
- [26] G. M. Rebeiz, *RF MEMS: theory, design, and technology*. John Wiley & Sons, 2004.
- [27] C. Providakis and D. Beskos, "Dynamic analysis of beams by the boundary element method," *Comput. Struct.*, vol. 22, no. 6, pp. 957–964, 1986.
- [28] F. Shi, P. Ramesh, and S. Mukherjee, "Dynamic analysis of micro-electro-mechanical systems," *Int. J. Numer. Meth. Eng.*, vol. 39, no. 24, pp. 4119–4139, 1996.
- [29] S. K. De and N. R. Aluru, "Full-lagrangian schemes for dynamic analysis of electrostatic mems," *J. Microelectromech. Syst.*, vol. 13, no. 5, pp. 737–758, 2004.



I. C. Benitez-Zuñiga was born in Mexico City, Mexico. He received his B. S. and M. Eng. Degrees in electrical and electronic engineering from the National Autonomous University of Mexico (UNAM), Mexico City in 2012 and 2016, respectively. Currently, he is pursuing a Ph. D. degree at the Faculty of Engineering, UNAM. Since 2012, he has been a professor at the National School College of Sciences and Humanities, Pre-University School, UNAM. His research interests include RF MEMS, phased array antennas and millimeter-wave devices.



millimeter-wave communications.

A. E. Martynyuk was born in Kiev, Ukraine. He received an M. Sc. Degree in radio engineering in 1988 from Kiev Polytechnic Institute, Ukraine, and Ph. D. degree in 1993 from same institute. Since 1988 to 1995, he was with the Faculty of Radio Engineering of the Kiev Polytechnic Institute. Since 1995 he has been with the National Autonomous University of Mexico (UNAM), Mexico City. He is currently a professor at the Faculty of Engineering, UNAM. His research interests include microwave and millimeter-wave devices, antenna arrays and



From 2019 to 2021, he was a Visiting Professor at the Nonlinear RF Laboratory, Department of Electrical and Computer Engineering, OSU. He is currently a professor of electrical engineering with UNAM. His current research interests include antenna arrays, frequency-selective surfaces, and microwave and millimeter wave circuits.



J. Rodriguez-Cuevas was born in Mexico City, Mexico. He received his B. S., M. Eng., and Ph. D. degrees in electrical engineering from the National Autonomous University of Mexico (UNAM), Mexico City, Mexico, in 1987, 1995 and 2003, respectively. Furthermore in 2003, he received specialized studies in Microelectromechanical Systems (MEMS) from the National Autonomous University of Mexico (UNAM) and the United States-Mexico Foundation for Science (FUMEC). Since 1987, he has been with the Electronics Engineering Department, UNAM, where he is a professor engaged in research and teaching on telecommunication circuits and systems. His current research interests are phased arrays, RF MEMS and microwave and millimeter-wave circuits.